Extreme Mechanics Letters 8 (2016) 245–250

Contents lists available at ScienceDirect

Extreme Mechanics Letters

journal homepage: www.elsevier.com/locate/eml

Ton-scale metal–carbon nanotube composite: The mechanism of strengthening while retaining tensile ductility

Kang Pyo So [a], Xiaohui Liu [a,b], Hideki Mori [c], Akihiro Kushima [a], Jong Gil Park [d], Hyoung Seop Kim [e], Shigenobu Ogata [f,g,*], Young Hee Lee [d,**], Ju Li [a,**]

[a] Department of Nuclear Science and Engineering and Department of Materials Science and Engineering, Massachusetts Institute of Technology, Cambridge, MA 02139, USA

[b] School of Materials Science and Engineering, Shanghai Jiao Tong University, Shanghai 200240, China

[c] Department of Mechanical Engineering, College of Industrial Technology, 1-27-1 Nishikoya, Amagasaki, Hyogo 661-0047, Japan

[d] IBS Center for Integrated Nanostructure Physics, Institute for Basic Science (IBS), Sungkyunkwan University 440-746, Republic of Korea

[e] Department of Materials Science and Engineering, Pohang University of Science and Technology, Pohang 790-784, Republic of Korea

[f] Department of Mechanical Science and Bioengineering, Osaka University, Osaka 560-8531, Japan

[g] Center for Elements Strategy Initiative for Structural Materials (ESISM), Kyoto University, Kyoto 606-8501, Japan

ARTICLE INFO

Article history:
Received 3 January 2016
Received in revised form 6 April 2016
Accepted 11 April 2016
Available online 28 April 2016

ABSTRACT

One-dimensional carbon nanotubes (CNT), which are mechanically strong and flexible, enhance strength of the host metal matrix. However, the reduction of ductility is often a serious drawback. Here, we report significantly enhanced plastic flow strength, while preventing tensile ductility reduction, by uniformly dispersing CNTs in Al matrix. Nanoscale plasticity and rupturing processes near CNTs were observed by *in-situ* mechanical tests inside Transmission Electron Microscope (TEM). CNTs act like forest dislocations and have comparable density ($\sim 10^{14}/m^2$), and such 1D nano-dispersion hardening is studied in detail by in situ TEM and molecular dynamics simulations. Rupture-front blunting and branching are seen with *in situ* TEM, which corroborates the result from macro-scale tension tests that our Al + CNT nanocomposite is quite damage- and fault-tolerant. We propose a modified shear-lag model called "Taylor-dispersion" hardening model to highlight the dual roles of CNTs as load-bearing fillers and "forest dislocations" equivalent that harden the metal matrix, for the plastic strength of metal + CNT nanocomposite.

In this paper we show how the Nano can impact the Macro at 10^3 kg level, fifteen years after the highly speculative concept of carbon nanotube (CNT) cables for space elevator was proposed [1]. Metal + CNT composites (MCC), specifically Aluminum + CNT composite, can now be mass produced (Fig. 1) at less than twice the cost of bulk Al (including raw material cost of CNTs and processing costs), with 150% the mechanical strength of Al but with no loss in tensile ductility (Fig. 2(a)). Analyzing its mechanism is the subject of this Letter, based on our *in situ* mechanical deformation experiments inside Transmission Electron Microscope (TEM), molecular dynamics (MD) simulations, and standard dislocation mechanics modeling. The shear lag models [2] commonly used for fiber-(polymer)matrix composites are unlikely to work very well here, as the CNTs are dispersed at approximately the same length scale as the dislocations, and therefore strengthen the composite not only by carrying the load themselves (direct effect, described by the shear lag model), but also by strengthen-

* Corresponding author at: Department of Mechanical Science and Bioengineering, Osaka University, Osaka 560-8531, Japan.
** Corresponding authors.
E-mail addresses: ogata@me.es.osaka-u.ac.jp (S. Ogata), leeyoung@skku.edu (Y.H. Lee), liju@mit.edu (J. Li).

http://dx.doi.org/10.1016/j.eml.2016.04.002
2352-4316/

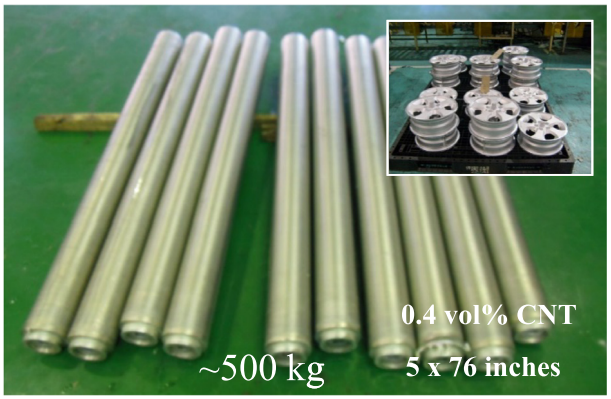

Fig. 1. A proof-of-concept of the mass produced Al + CNT composite. As-cast Al + CNT composite billet with 0.4 vol% CNT, inset: Al + CNT wheels.

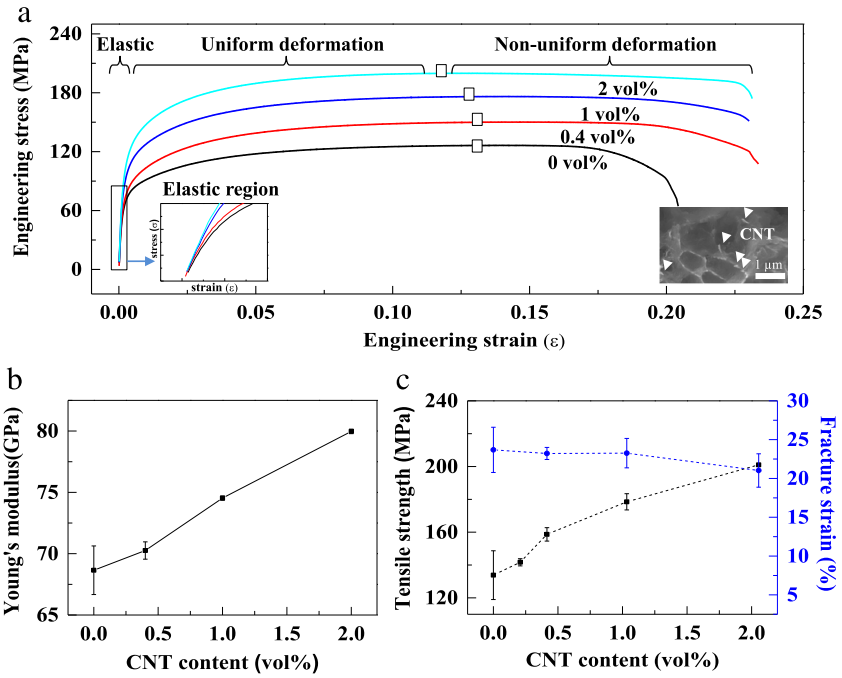

Fig. 2. Mechanical properties of Al + CNT composite after powder metallurgy and extrusion. (a) The stress vs. strain curves for different CNT contents (ASTM E8 tensile specimen). (b) Young's modulus (c) tensile strength and fracture strain at different CNT contents.

ing the metal matrix through 1D nano-dispersion hardening (indirect effect, based on size-dependent metal plasticity [3]).

Individual CNTs possess the ultimate mechanical properties, for example, ~1TPa Young's modulus, 100 GPa level tensile strength, nm-scale diameters, high bending flexibility and large surface area [4]. Dispersing CNTs in metals has an aesthetic appeal, because both dislocations and CNTs are flexible 1D microstructures in the metal matrix. As far as mobile dislocations are concerned, CNTs act pretty much as impenetrable "forest dislocations" (see our MD simulations below), so CNT-induced strengthening *of the metal* should be similar to the Taylor hardening mechanism:

$$\Delta\sigma_{\text{metal}} = A\mu b\left(B\rho_{\text{CNT}} + \rho\right)^{1/2}, \tag{1}$$

where σ_{metal} is the flow stress of the metal matrix, μ is the metal's shear modulus, b is its full Burgers vector length, ρ and ρ_{CNT} are the total length of dislocations and CNTs per volume (with the same unit of $1/\text{m}^2$), and A, B are dimensionless constants on the order of 1, where B converts CNT line length to an equivalent dislocation line length. A rough order of magnitude can be estimated on how much CNTs would be needed for significant strengthening, if we assume $B = 1$ and $\rho_{\text{CNT}} = \rho$. A baseline level of dislocation density in well-annealed metal is $\rho = 10^{12}/\text{m}^2$. A mediumly cold-worked face-centered cubic (FCC) Cu has dislocation density $\rho = 4 \times 10^{14}/\text{m}^2$. The dislocation density upper bound that can be reached through severe plastic deformation is of the order $\rho_{\max} \sim 10^{16}/\text{m}^2$ [5–8]. If we assume CNT radius $r \sim 10^{-9}$ m, we

get an estimated volume fraction of CNT

$$\phi_{CNT} = \rho_{CNT}\pi r^2, \quad (2)$$

that ranges between 0.1% (corresponding to mediumly cold-worked FCC Cu) to 3% (corresponding to dislocation density upper bound [5], ρ_{max}), which is right within the range of processing and economy: that is, ϕ_{CNT} is not so big that the raw cost of CNT dominates over the bulk metal cost. So, here we have a case of carbon nanotubes meeting physical metallurgy, which intriguingly was not for the first time [9].

It is important to note that Eq. (1) is a lengthscale-aware plasticity model *on the metal side*. To get the composite strength, one needs to take into account the load-bearing capabilities of both the metal (volume fraction $1 - \phi_{CNT}$) and the CNTs (volume fraction ϕ_{CNT}), where σ_{metal} is the strength of metal matrix and σ_{CNT} is the strength of CNTs.:

$$\sigma_{composite} = f(\sigma_{metal}, \sigma_{CNT}, \phi_{CNT}). \quad (3)$$

For ϕ_{CNT} of less than a few percent, however, it is a reasonable approximation to write

$$\Delta\sigma_{composite} \approx \Delta\sigma_{shear\ lag} + \Delta\sigma_{metal}, \quad (4)$$

where $\Delta\sigma_{shear\ lag}$ is contributed by the transfer of stress from matrix to fiber by means of interfacial shear stresses and can be expressed as $\sigma_{metal}(1 - \phi_{CNT}) + C\sigma_{CNT}\phi_{CNT}$ using the conventional shear lag model for fiber-matrix composites *without size effect* in the constitutive law for the matrix, and $\Delta\sigma_{metal}$ comes from Eq. (1), which treats the dispersion strengthening due to 1D CNTs as the equivalent forest dislocation strengthening.

One common issue in CNT-reinforced metal composites is the reduced ductility when mechanical strength is enhanced. This trend becomes even more severe when the dispersion of CNTs is poor [10]. The reduction of ductility has been prevented by improving dispersion and wetting of CNTs in Al matrix [9,10]. However, the underlying mechanism has not been analyzed carefully.

Typical stress–strain curves for samples with different ϕ_{CNT} are shown in Fig. 2(a). The curves are divided into uniform and non-uniform elongation regimes separated by the necking point based on the Considère criterion [11]. (Figs. S1a and b). The maximum engineering stress (tensile strength) increases in proportional to ϕ_{CNT}, while the uniform elongation strain is slightly reduced. The fracture strains are not degraded appreciably even for high CNT concentration (up to 2 vol% CNT). Young's modulus also increases in proportional to ϕ_{CNT}, which is a clear evidence of efficient load transfer (Figs. 2(a), left inset and 2(b)) [12]. The broken CNTs in the fracture area indicate the efficient load transfer at the interface (right inset in Fig. 2(a)). TEM observations confirm that CNTs are dispersed inside Al grains and not just along the grain boundaries, as shown in Fig. 3(a). The structural state of CNTs in Al grain are characterized by Raman spectra in Fig. 3(b). Although a broad D band, indicating the structural damage of CNTs during dispersion process, is observed after fabrication of the composite, the presence of sharp G band verifies graphitic sp^2 carbons. A slight upshift of the G band is ascribed to the doping effect caused by the formation of interfacial chemical bonds (Fig. 2(d)) [13]. Confocal Raman mapping of G band further demonstrates that relatively fine dispersion of CNTs is achieved throughout the whole Al matrix (Fig. 3(c)) [14]. Taking $\phi_{CNT} = 0.02$ and $r = 7.5$ nm for the multi-walled CNTs used here, ρ_{CNT} has an order of magnitude of 10^{14} m^{-2}, which is comparable to the measured dislocation density of cold worked FCC metal. The CNTs (ρ_{CNT}) may also have similar degree of fractal aggregation as the dislocations (ρ) at μm resolution [15]. The two fundamental criteria for making a high-performance composite [16], good dispersion and interfacial strength, should be reasonably satisfied here. The relationship between tensile strength and fracture strain for different CNT concentration is shown in Fig. 2(c). The CNTs in the composite significantly improve the tensile strength (for example, 50.2% enhancement at 2 vol% CNT), while maintaining the fracture strain.

The comparable magnitude of ρ_{CNT} and ρ implies high possibility of interaction between dislocations and CNTs in our materials, as these 1D string defects are co-mixed together. *In-situ* TEM observation on deformation of the Al + CNT composite clearly verified that CNTs can resist dislocation motion, as shown in Fig. 4(a)–(d) (see experimental details and video S1 in supplementary, Appendix A). Under tensile deformation, a dislocation splits into α and β, moving towards a CNT nearby (Fig. 4(a) and (b)). The dislocation α is first pinned by the CNT while β keeps moving (Fig. 4(c)), and eventually both dislocations are pinned (Fig. 4(d)). Further evidence of multiple dislocations pinning by CNTs can be found in Fig. S4 (see Appendix A).

We used molecular dynamics simulation to study the interaction between a discrete dislocation and a CNT under shear stress (Fig. S5, Appendix A). Fig. 4(e) shows a snapshot whereby an edge dislocation driven by shear stress meets a CNT 1.5 nm in diameter. Unlike conventional nano-sized precipitates (0D) in Al alloys, CNTs cannot be sheared through by dislocations, due to the high strength of C–C bonding and bending flexibility of the tube. Furthermore, due to the large aspect ratio of CNTs, it would be extremely difficult for dislocations to bypass the 1D CNTs by dislocation climb, or cross slip of screw segments (Video S2, Appendix A) [17]. Consequently, simple Orowan looping would be the dominant mechanism for dislocation bypassing of CNTs. As a result, the increase of the yield strength of our Al + CNT composites can be formulated by the Orowan model [18] (see Fig. S6 for details), which actually fits the experimental data well up to 4 vol% (Fig. 4(f)). Deviation for higher CNT concentration probably originates from the limited dispersion ability of CNTs within the Al matrix, as CNTs may become even more fractally aggregated [15].

The uniform elongation and ultimate tensile strength of our Al + CNT composites are compared with other materials, including pure Al, Al alloys with precipitates [19,20] and other Al + CNT composites [21–27], as shown in Fig. 5(a). It is clear that Orowan looping increases the resistance to dislocation motion, which accounts for the improved strength of our composites over the pure Al. Besides, compared with other Al/CNTs composites, the uniform elongation does not degrade significantly even for high concentration of CNTs. This can be attributed to

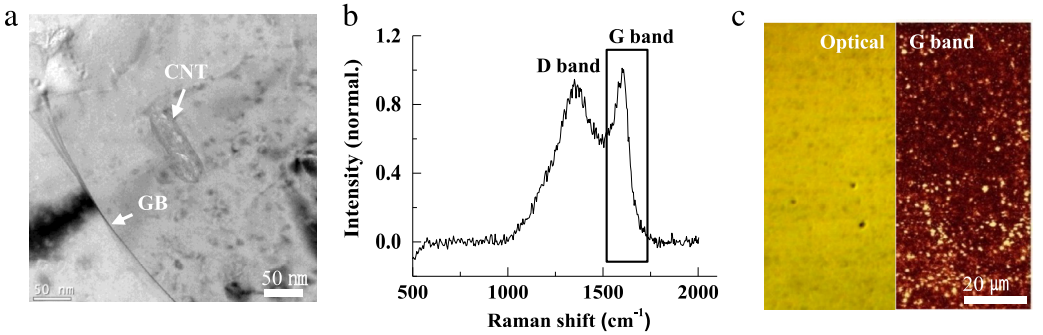

Fig. 3. Dispersion of CNT in Al matrix. (a) Dispersion of CNT inside Al grains in TEM. (b) Raman spectra of Al + CNT composite and (c) confocal Raman mapping image of G band.

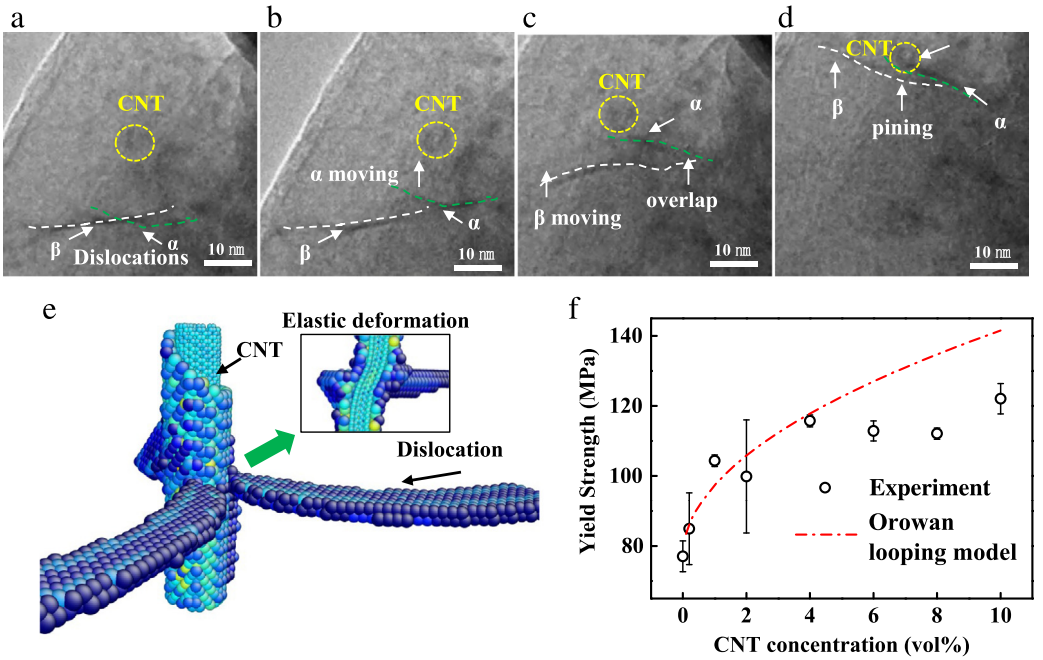

Fig. 4. The observation and simulation of the dislocation pinning by CNT. *In-situ* TEM observation of dislocation pinning by CNT under deformation: (a) location of CNT and two dislocations, (b) dislocation splits into α and β after deformation. (c) Dislocation α is pinned by CNT while β keeps moving, (d) both dislocations are pinned by CNT. (e) MD simulation of the dislocation pinning and (f) comparison of the yield strength improvement between Orowan looping model calculation and experiments. The detailed parameter for *in-situ* observation and MD simulation are described in Supplementary (see Appendix A).

the enhanced strain hardening rate $\frac{\partial\sigma}{\partial\varepsilon}\big|_{\dot{\varepsilon}}$ (Fig. 5(b)), as evidenced by the increase of the micro-strain of the post-elongation samples measured with X-ray diffraction (XRD) (Fig. S7, Appendix A), resulting from better dispersion of CNTs inside the Al grains [28] and thus more dislocation accumulation due to co-mixing and pinning by CNTs that retard dislocation recovery.

Unlike non-shearable precipitates [29], CNTs are elastically flexible, which alleviates lattice mismatch near the Al–CNTs interfaces. This is verified by our direct MD simulation of multiple dislocation bypassing of a CNT (Fig. S8, Appendix A). Although CNT becomes more resistive to surrounding plastic flow after undergoing significant shear strain due to its nonlinear elasticity, the actual deformation is somewhat localized in the vicinity of the slip plane, and the rest of the CNT still remains flexible.

The non-uniform elongation and rupturing were studied under *in-situ* deformation TEM (see supplementary for the details of sample preparation and the holder). We observed and analyzed the role of CNTs during rupturing. A rupture front is generated on the surface of the sample after slight necking under 25% tensile deformation (Fig. S9). It continuously propagates inwards under tension till prevented by a CNTs cluster, and further tension blunts it. Subsequently, a 2nd rupture front initiates and propagates alongside the CNTs zone (Fig. S9), and a 3rd rupture front is generated on the other side before the final fracture (see Appendix A). We then plot the length of the first two rupture fronts versus the opening displacement in Fig. 6(a). The propagation of the 1st rupture tip becomes faster as displacement increases. However, the CNTs cluster blocks its further propagation, and later generation of the 2nd front extends the damage. This event will create

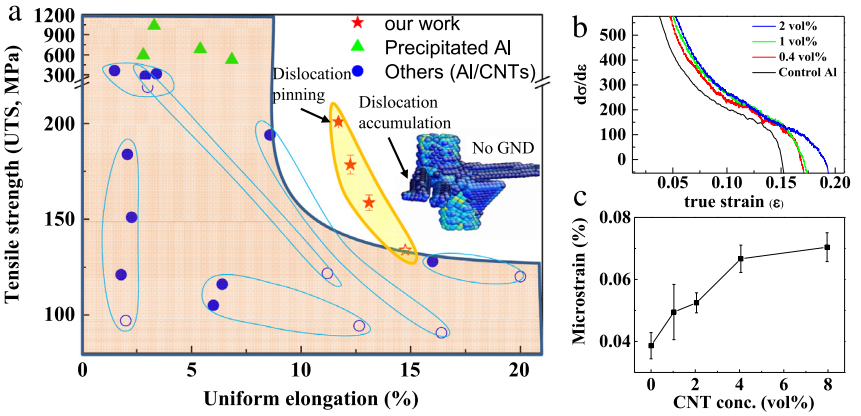

Fig. 5. Improvement of necking point and strain hardening rate. (a) Tensile strength versus uniform elongation. The data are compared with previously published Al + CNT composite and precipitation hardened Al. Each processes are grouped in light blue ellipses. The open circle indicates the control pure Al in the process. (b) Strain hardening rate ($d\sigma/d\varepsilon$). Higher concentration of CNTs induces higher strain hardening. (c) X-ray diffraction measured microstrain broadening at different CNT content. (For interpretation of the references to color in this figure legend, the reader is referred to the web version of this article.)

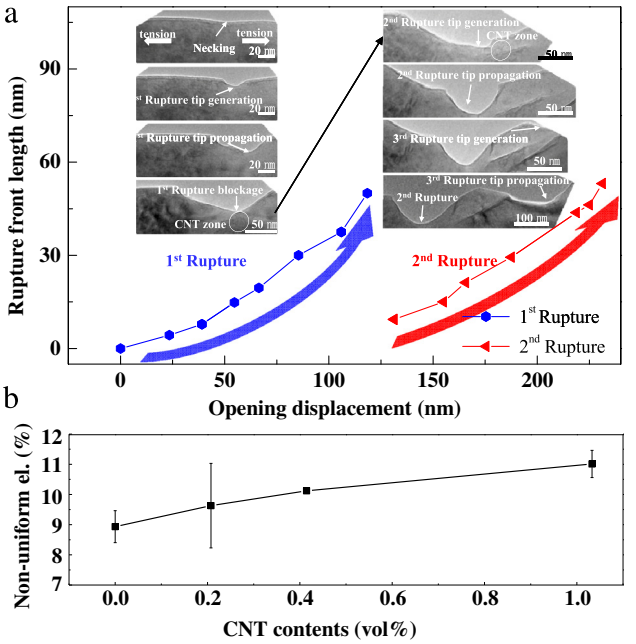

Fig. 6. *In-situ* TEM observation of the rupturing process. (a) Rupture front length vs opening displacement at rupture. CNTs cluster make rupture tip split into two. The generation and propagation of 1st and 2nd rupture tip are indicated in the inset. (b) Non-uniform elongation at different CNT content. Higher CNT content increases the non-uniform elongation.

the major rupture/crack split, resulting in the delaying of the fracture, which explains the non-uniform elongation on the bulk tensile test increasing with higher content of CNTs, as shown in Fig. 6(b). Such damage-tolerant feature is quite rare in small-scale samples, after sustaining sample size-dependent hardening, which corroborates the result from macro-scale tests that our Al + CNT nanocomposite is quite damage- and fault-tolerant in tension.

In conclusion, we found that well-dispersed CNTs inside Al grain improve strength without sacrificing ductility. The mechanisms are investigated by MD simulation and *in-situ* TEM tensile rupture tests. The MD simulation verifies CNTs serve as impenetrable 1D nano-dispersions, inducing dislocation accumulation in front of and around CNTs. This contributes to strain hardening. Based on the above, we propose a composite strength model Eqs. (1)–(4), hereon named "Taylor-dispersion hardening" model, to highlight the dual roles of CNTs as load-bearing fillers and "forest dislocations" equivalent that harden the metal matrix, for the plastic flow strength of metal + CNT nanocomposites. We also demonstrate that non-uniform elongation was improved by multi-step rupturing process after necking point, by observing the microscopic damage evolution, that indicates rupturing front jumps. The retained tensile ductility on top of significantly enhanced strength is attributed to good dispersion and interfacial strength of the embedded CNTs, which are 1D nano-dispersions akin to forest dislocations.

Acknowledgments

We acknowledge support by National Science Foundation (NSF) DMR-1410636, DMR-1120901, ESISM Japan and JSPS KAKENHI (Grant Nos. 22102003, 23246025, and 25630013). This work was also supported by the Research Center Program of IBS (IBS-R011-D1).

Appendix A. Supplementary data

Supplementary material related to this article can be found online at http://dx.doi.org/10.1016/j.eml.2016.04.002.

References

[1] B.C. Edwards, Design and deployment of a space elevator, Acta Astronaut. 47 (2000) 735–744. http://dx.doi.org/10.1016/s0094-5765(00)00111-9.
[2] S.R. Bakshi, D. Lahiri, A. Agarwal, Carbon nanotube reinforced metal matrix composites—a review, Int. Mater. Rev. 55 (2010) 41–64. http://dx.doi.org/10.1179/095066009X12572530170543.
[3] T. Zhu, J. Li, Ultra-strength materials, Prog. Mater. Sci. 55 (2010) 710–757. http://dx.doi.org/10.1016/j.pmatsci.2010.04.001.
[4] M.F. Yu, et al., Strength and breaking mechanism of multiwalled carbon nanotubes under tensile load, Science 287 (2000) 637–640. http://dx.doi.org/10.1126/science.287.5453.637.
[5] J. Gil Sevillano, in: Vicente Amigó Borrás (Ed.), International Symposium on Plastic Deformation and Texture Analysis, Universitat Politècnica de València, 2012, pp. 25–38.
[6] J. Gil Sevillano, Substructure and strengthening of heavily deformed single and two-phase metallic materials, J. Phys. III France 1 (1991) 967–988.
[7] R.Z. Valiev, R.K. Islamgaliev, I.V. Alexandrov, Bulk nanostructured materials from severe plastic deformation, Prog. Mater. Sci. 45 (2000) 103–189. http://dx.doi.org/10.1016/S0079-6425(99)00007-9.
[8] A.P. Zhilyaev, T.G. Langdon, Using high-pressure torsion for metal processing: Fundamentals and applications, Prog. Mater. Sci. 53 (2008) 893–979. http://dx.doi.org/10.1016/j.pmatsci.2008.03.002.
[9] M. Reibold, et al., Materials: Carbon nanotubes in an ancient Damascus sabre, Nature 444 (2006) 286. http://www.nature.com/nature/journal/v444/n7117/suppinfo/444286a_S1.html.
[10] D. Lahiri, S.R. Bakshi, A.K. Keshri, Y. Liu, A. Agarwal, Dual strengthening mechanisms induced by carbon nanotubes in roll bonded aluminum composites, Mater. Sci. Eng. A-Struct. 523 (2009) 263–270. http://dx.doi.org/10.1016/j.msea.2009.06.006.
[11] G.E. Dieter, D. Bacon, Mechanical Metallurgy, McGraw-Hill, 1988.
[12] K.K. Chawla, Composite Materials: Science and Engineering, Springer Science & Business Media, 2012.
[13] K.P. So, et al., Improving the wettability of aluminum on carbon nanotubes, Acta Mater. 59 (2011) 3313–3320. http://dx.doi.org/10.1016/j.actamat.2011.01.061.
[14] K.P. So, et al., Dispersion of carbon nanotubes in aluminum improves radiation resistance, Nano Energy 22 (2016) 319–327.
[15] P. Hähner, K. Bay, M. Zaiser, Fractal dislocation patterning during plastic deformation, Phys. Rev. Lett. 81 (1998) 2470–2473.
[16] S. Hao, et al., A transforming metal nanocomposite with large elastic strain, low modulus, and high strength, Science 339 (2013) 1191–1194. http://dx.doi.org/10.1126/science.1228602.
[17] D. Hull, D.J. Bacon, Introduction to Dislocations, fifth ed., Elsevier Science, 2011.
[18] E. Orowan, Discussion in The Symposium on Internal Stresses in Metals and Alloys, Inst. Metals, London, 1948, p. 451.
[19] Y.H. Zhao, X.Z. Liao, S. Cheng, E. Ma, Y.T. Zhu, Simultaneously increasing the ductility and strength of nanostructured alloys, Adv. Mater. 18 (2006) 2280–2283. http://dx.doi.org/10.1002/adma.200600310.
[20] P.V. Liddicoat, et al., Nanostructural hierarchy increases the strength of aluminium alloys, Nature Commun. 1 (2010) 63. http://dx.doi.org/10.1038/Ncomms1062.
[21] L. Jiang, Z.Q. Li, G.L. Fan, L.L. Cao, D. Zhang, Strong and ductile carbon nanotube/aluminum bulk nanolaminated composites with two-dimensional alignment of carbon nanotubes, Scr. Mater. 66 (2012) 331–334. http://dx.doi.org/10.1016/j.scriptamat.2011.11.023.
[22] J. Stein, B. Lenczowski, N. Frety, E. Anglaret, Mechanical reinforcement of a high-performance aluminium alloy AA5083 with homogeneously dispersed multi-walled carbon nanotubes, Carbon 50 (2012) 2264–2272. http://dx.doi.org/10.1016/j.carbon.2012.01.044.
[23] J. Wu, H. Zhang, Y. Zhang, X. Wang, Mechanical and thermal properties of carbon nanotube/aluminum composites consolidated by spark plasma sintering, Mater. Des. 41 (2012) 344–348.
[24] H. Kwon, M. Leparoux, Hot extruded carbon nanotube reinforced aluminum matrix composite materials, Nanotechnology 23 (2012) 415701.
[25] H. Kwon, M. Estili, K. Takagi, T. Miyazaki, A. Kawasaki, Combination of hot extrusion and spark plasma sintering for producing carbon nanotube reinforced aluminum matrix composites, Carbon 47 (2009) 570–577. http://dx.doi.org/10.1016/j.carbon.2008.10.041.
[26] R. Pérez-Bustamante, et al., Microstructural and mechanical characterization of Al–MWCNT composites produced by mechanical milling, Mater. Sci. Eng. A 502 (2009) 159–163.
[27] J.G. Park, D.H. Keum, Y.H. Lee, Strengthening mechanisms in carbon nanotube-reinforced aluminum composites, Carbon 95 (2015) 690–698.
[28] K.P. So, Achieving both high ductility and mechanical strength in carbon nanotubes-reinforced Al, 2016.
[29] Y. Zhao, X. Liao, S. Cheng, E. Ma, Y. Zhu, Simultaneously increasing the ductility and strength of nanostructured alloys, Adv. Mater. 18 (2006) 2280–2280.